Estuaries and Coasts (2023) 46:1375–1386
https://doi.org/10.1007/s12237-023-01211-z

SHORT COMMUNICATION

Extension of the Practical Salinity Scale to Estimate Major Ion Concentrations: Application to the San Francisco Estuary

Paul H. Hutton[1] · **Sujoy B. Roy**[1]

Received: 21 October 2022 / Revised: 19 April 2023 / Accepted: 24 April 2023 / Published online: 27 June 2023

Abstract

This paper presents a novel approach to estimate major ion concentrations in estuaries from a known specific conductance. Assuming two-source conservative mixing at steady state, we propose an extension of the Practical Salinity Scale 1978 to estimate concentrations of major ions and total dissolved solids as functions of the conductivity ratio, which is the ratio of sample conductivity and seawater conductivity. We employ an extensive salinity data set that includes measurements of specific conductance and concentrations of major ions and total dissolved solids to demonstrate its validity and limitations for the San Francisco estuary. We show the proposed extension to be valid in waters influenced by seawater intrusion at specific conductance values greater than or equal to 0.25 mS/cm and propose adjusted model constants to account for ionic composition under less saline conditions. We observed evidence of seasonal bias in model residuals and hypothesize that this bias is related to the simplified assumption of fixed upstream end member concentrations. This finding of seasonal bias suggests that upstream end member concentrations are more reflective of high alkalinity freshwater contributions from December through June, compared to other months.

Keywords Salinity constituents · Estuarine water quality · Conservative mixing · Seawater intrusion

Introduction

The salinity gradient resulting from mixing of ocean water and riverine water is a fundamental feature of estuaries and affects biota within the system as well as surrounding marine waters (Reid and Wood 1976; Telesh and Khlebovich 2010). The salinity gradient also plays a role in municipal and agricultural uses of estuarine waters, i.e., water withdrawals generally occur in the more upstream reaches of an estuary where salinities are lower. Estuarine salinity gradients are affected by several factors, including geometry, volumes, and timing of freshwater inflows, tidal ranges, and wind-driven mixing (Dyer 1997). Some of these factors are subject to change over longer time scales due to anthropogenic drivers; common drivers include water diversions, dredging and filling activities, tidal wetland loss, and sea level rise (Merrifield et al. 2011; Kennish 2021). While estuarine mixing studies typically focus on the state and transport of bulk salinity measures, many studies consider the state and transport of individual ions that are of interest for specific beneficial uses (Yarish et al. 1980; Howland et al. 2000; Sundaray et al. 2009; Carol and Kruse 2012; Denton 2015).

The most common measure of salinity in estuarine waters is electrical conductivity because of the widespread use of real-time sensors that can easily provide time-varying data. Conductivity is related to salinity through the Practical Salinity Scale 1978 (PSS-78) (Lewis 1980), an empirical relationship expressing salinity in dimensionless units with a value of 35 referring to ocean water salinity. Conductivity measurements for estuarine waters are usually converted to a standard temperature and pressure (25 °C and 1 atmosphere) and reported as specific electrical conductance (EC). The use of PSS-78 for estimating total salinity has been commonplace after publication in Lewis (1980).

Here, we build on the standard PSS-78 formulation by proposing similar relationships between EC and individual ionic concentrations to extend the utility of EC measurements. We focus on San Francisco estuary, including the western Sacramento-San Joaquin River Delta (hereafter Delta), a region with abundant ionic and EC data and where

Communicated by Dennis Swaney

✉ Sujoy B. Roy
sujoy.roy@tetratech.com

[1] Tetra Tech, Lafayette, CA, USA

an ongoing interest in ionic composition is motivated by several regulatory and drinking water quality considerations, including:

- Water quality regulations (CSWRCB 1999) governing the operation of Delta facilities by the California State Water Project (SWP) and Federal Central Valley Project (CVP) set chloride standards at various intakes to protect municipal and industrial beneficial uses.
- Salinity intrusion introduces ocean-derived bromide salts to the interior Delta (Hutton and Chung 1992). This salinity ion is of special concern for municipal beneficial uses of Delta water, as it promotes the formation of several disinfection by-products that are suspected threats to human health when present in sufficient quantities in drinking water (Najm and Krasner 1995). Bromine-containing disinfection by-products are of greater health concern than their chlorine-containing analogs (Wagner and Plewa 2017).
- Concerns about low alkalinity levels in exported Delta waters have been raised by SWP contractors that serve municipalities, prompting the California Department of Water Resources' Municipal Water Quality Investigations (MWQI) program to develop capabilities to simulate and forecast bicarbonate fate and transport in the Delta (Hutton et al. 2022a). While moderately low alkalinity levels can improve the effectiveness of the coagulation process in water treatment plants, especially when aluminum sulfate is used as a coagulant, extremely low alkalinity levels can depress pH levels and can result in re-stabilization of organic carbon (Krasner and Amy 1995).
- SWP contracts for water supply contain water quality objectives for several salinity constituents, including total dissolved solids, total hardness, chloride, sulfate, and sodium. The State of California agreed to take all reasonable measures to make available SWP water to its contractors that does not exceed specific concentration limits for these constituents (for example, see CDWR 2003).

Assuming two-source conservative mixing at steady state (a seawater source and a freshwater source), we extend the PSS-78 formulation to estimate individual ionic concentrations as a function of EC. We employ a salinity data set that includes co-located measurements of EC and concentrations of major ions and total dissolved solids to demonstrate its validity and limitations for the San Francisco estuary. We show the proposed extension to be valid in waters influenced by seawater intrusion at specific conductance values greater than or equal to 0.25 mS/cm and propose adjusted model constants to account for ionic composition under less saline conditions. This methodology is adaptable to other estuaries with a single freshwater source and can easily account for a freshwater ionic signature that is different from that of ocean water.

Methods

Background

Study Area

The salinity gradient in San Francisco estuary, influenced by California's Mediterranean climate and altered to support human beneficial uses, has been a focus of study for nearly a century (California Department of Public Works 1931; Hutton et al. 2015). Figure 1 shows a truncated map of San Francisco estuary; this map (which excludes most of the Sacramento-San Joaquin River Delta) identifies the confluence of the major riverine inflows at its upstream boundary as well as the location of the downstream bays relative to the Pacific Ocean. Freshwater flow to the estuary is highly seasonal, with most of the volume occurring from November through June. As a result of this flow pattern, the salinity gradient is also strongly seasonal, with greater salinity intrusion during the dry months of July through October (Hutton et al. 2015). The zone in which freshwater mixes with seawater in the estuary extends upstream, as well as seaward, from the confluence of the Sacramento and San Joaquin Rivers. For purposes of this work, we define the approximate upstream boundary of the study area as Emmaton along the Sacramento River and Jersey Point along the San Joaquin River.

The estuary's salinity gradient is regulated through management of water discharges from reservoirs and freshwater withdrawals for agricultural and municipal use (CSWRCB 1999). While contemporary management has typically focused on total salinity, expressed in the form of specific electrical conductance (EC), interest in the concentrations of total dissolved solids (TDS) and individual major ions also exists, as these measures are related to regulatory standards and potential uses of these waters for municipal supply (Denton 2015). Empirical quadratic relationships between EC, total dissolved solids, and major ions have been developed for different regions of the estuary to inform these interests (Denton 2015; Hutton et al. 2022b).

Practical Salinity Scale

The Practical Salinity Scale 1978 (Lewis 1980) is widely used as a conductivity-based measure of salinity in oceans and estuaries. The scale produces a dimensionless quantity that is defined as a function of a conductivity ratio (sample conductivity divided by seawater conductivity), temperature, and pressure. The scale, by definition, returns a value of 35 for seawater with a conductivity ratio of unity. Lewis (1980) reports that the scale is valid over the range of 2 to 42. Hill et al. (1986) presents a standard correction to the scale to extend

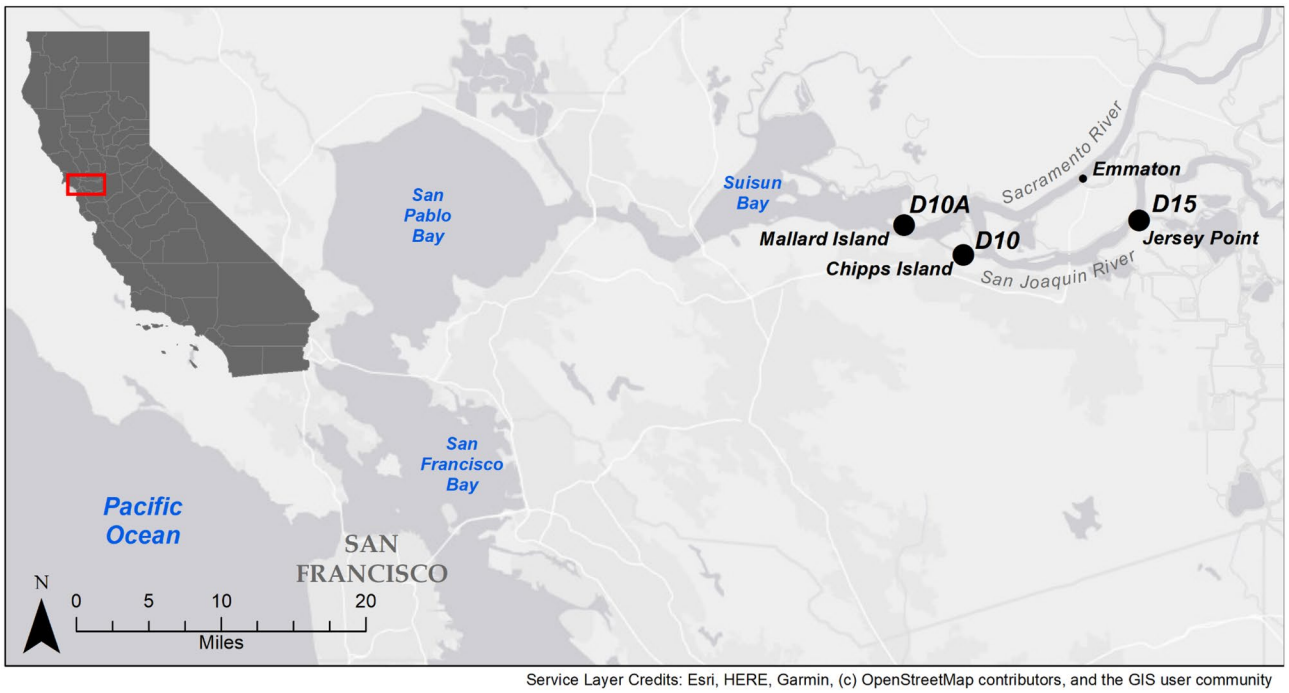

Fig. 1 Map of San Francisco estuary with the Sacramento-San Joaquin River confluence as the upstream boundary

the applicability of PSS-78 below a value of 2. This correction is based on dilutions of standard seawater with pure water and thus is strictly applicable to waters that have the same proportional ionic makeup as standard seawater. Hutton and Roy (in review) found the scale to be valid in the study area at practical salinity values as low as 0.06 (0.12 mS/cm EC).

Noting that conductivity data are typically collected in the study area at shallow depths and are normalized to a standard temperature of 25 °C, Schemel (2001) presents the following simplified version of PSS-78 assuming a standard temperature and atmospheric pressure:

$$S = K_o + K_1 * R^{0.5} + K_2 * R + K_3 * R^{1.5} + K_4 * R^2 + K_5 * R^{2.5} \quad (1)$$

where $K_o = 0.0120$, $K_1 = -0.2174$, $K_2 = 25.3283$, $K_3 = 13.7714$, $K_4 = -6.4788$, $K_5 = 2.5842$, $\sum K = 35$, and R is a conductivity ratio which is defined as the sample conductance divided by seawater conductance.

Conservative Mixing in Estuaries

Plots of dissolved constituents versus salinity, or "mixing diagrams," are commonly used to evaluate adherence to conservative mixing behavior in estuaries. Maeda (1952) used mixing diagrams to demonstrate linear (and thus conservative) relationships between silicate and chloride in several estuaries in Japan. Silicate, unlike ionic constituents that constitute salinity, is a dissolved constituent that is characterized by high concentrations in riverine source waters and low concentration in ocean water. Boyle et al. (1974) tabulated a literature review of early efforts following Maeda (1952) to study conservative mixing processes in estuaries; the emphasis of most of these early studies was on silicate. Subsequently, the mixing diagram approach has been used to study mixing behavior of other conservative and non-conservative constituents (for example, see Warner 1972; Boyle et al. 1974; Wong 1979; Loder and Riechard 1981; Kimmerer 2005; Patra et al. 2012; Cloern et al. 2017; Najjar et al. 2019; Zhang et al. 2020).

Cloern et al. (2017) point out that the mixing diagram approach "… is informative and appealing because of its simplicity, exploiting differences in the chemical and physical properties of seawater and freshwater." In general, the spatial structure of a conservative constituent is determined by steady state mixing of the two end members (i.e., upstream freshwater and downstream seawater), and concentration varies linearly along the salinity gradient. Interpretation of steady state conservative mixing behavior can be complicated by factors such as (i) the presence of intermediate sources or sinks and (ii) temporal variability in end member concentrations on time scales of estuary flushing (Loder and Reichard 1981; Najjar et al. 2019). These complicating factors aside, demonstration of non-linear behavior through mixing diagrams suggests non-conservative behavior of the constituent in question.

Data

Grab sample data collected from waters in the study area were used to evaluate the proposed extension of PSS-78 to estimate major ion concentrations. All data are measurements of surface conditions. In addition to specific conductance (EC), these data include concentrations of total dissolved solids (TDS); anions such as bromide (Br^-), chloride (Cl^-), sulfate (SO_4^{2-}), and alkalinity; and cations such as sodium (Na^+), calcium (Ca^{2+}), magnesium (Mg^{2+}), and potassium (K^+). EC values are reported in SI units of microsiemens per cm (µS/cm) and TDS and ion concentrations are generally reported in concentration units of mg/L. Alkalinity data are reported as mg/L of calcium carbonate.

Table 1 summarizes the number of grab sample data used in this work by constituent and location; this table also indicates the periods in which these data were collected. Data from monitoring locations near the confluence of the Sacramento and San Joaquin Rivers (D10A, D10, and D15) were collected and continue to be collected by the California Department of Water Resources (CDWR) in support of its Municipal Water Quality Investigations program (Hutton et al. 2022a). A subset of data collected by the program at the river confluence locations, along with data representing miscellaneous Bay locations downstream of the river confluence, were compiled from CDWR's Water Data Library http://www.water.ca.gov/waterdatalibrary/ to represent the study area. As indicated in Table 1, data from the three confluence monitoring locations are limited to samples with EC less than approximately 20,000 µS/cm. Complementing these data, data from the miscellaneous downstream locations represent samples with EC ≥ 20,000 µS/cm.

Denton (2015) notes that the quality of salinity grab sample data in the study area is generally very good and the robustness of correlations between various ionic constituents and EC at many locations within the study area allows for easy identification of data outliers and errors. We adhered to the following protocol to screen outliers:

- Grab sample data from monitoring locations D10A, D10, and D15 were checked for "testability." A testable data sample was defined as one that had a measured value for EC, TDS, Cl^-, SO_4^{2-}, Na^+, and Mg^{2+}. Testability was enforced to ensure that samples were generally mass- and charge-balanced.
- Following the check for "testability," two additional screening criteria were imposed: (i) a data point associated with a single constituent was removed if, when plotted against EC or TDS, fell outside the 99% prediction band (three standard errors) for the testable set of observations for that constituent and (ii) an entire sample, including all data points associated with it, was removed

Table 1 Number of specific conductance, TDS, and ion data points by monitoring location

Salinity constituent	Sac. R. @ Mallard (D10A) 1986–2019		Sac. R. @ Chipps (D10) 2019–2019		SJR @ Jersey (D15) 1990–1995		Miscellaneous Bay Locations[a] 1957–1973		Σ		Data range for locations D10A, D10, and D15
	EC ≥ 250 µS/cm	EC < 250 µS/cm	EC ≥ 250 µS/cm	EC < 250 µS/cm	EC ≥ 250 µS/cm	EC < 250 µS/cm	EC ≥ 250 µS/cm	EC < 250 µS/cm	EC ≥ 250 µS/cm	EC < 250 µS/cm	
EC	325	57	0	3	19	1	219	0	563	61	117 – 18,232
TDS	325	56	0	3	19	1	87	0	431	60	67 – 11,630
Bromide	280	55	0	3	19	1	0	0	299	59	0.01 – 20
Chloride	324	57	0	3	19	1	203	0	546	61	7 – 6,044
Sulfate	320	57	0	3	19	1	0	0	339	61	6 – 853
Alkalinity	319	57	0	3	19	1	60	0	398	61	37 – 96
Sodium	321	57	0	3	19	1	0	0	340	61	7 – 3,298
Calcium	322	57	0	3	19	1	0	0	341	61	8 – 143
Magnesium	317	57	0	3	19	1	0	0	336	61	4 – 424
Potassium	320	57	0	3	19	1	0	0	339	61	0.9 – 134

[a]These samples include data from the following locations downstream of the Sacramento and San Joaquin Rivers confluence: Fort Point, San Pablo Bay near Rodeo, San Pablo Bay near Point Davis, Suisun Bay at Bulls Head (D6), Sacramento River at Martinez (D6A), and Suisun Bay at Benicia (End-Pier). Data from these locations were limited to samples with EC ≥ 20,000 µS/cm

if three or more constituents in that sample fell outside the 95% prediction band (two standard errors) for the testable set of observations for the constituents.

The above screening is based on the assumptions that, while total salinity can exhibit unusual behavior under extreme hydrologic conditions, (i) relationships between individual constituents and total salinity exhibit consistent behavior for that region and (ii) major departures from these relationships are indicative of outlier behavior. Grab sample data from miscellaneous Bay locations downstream of the river confluence were not subjected to the above screening due to the limited number of constituents measured at these locations (EC, TDS, Cl^-, and alkalinity).

Results

We adopt the conceptual model of steady state two-source conservative mixing to develop an extension of PSS-78 for predicting major ion concentrations from a known conductivity ratio. As summarized below, we first derive generalized linear relationships between ion concentrations and salinity based on conservative mixing assumptions; these relationships are then substituted into the PSS-78 equation—i.e., Eq. (1)—to derive ion-specific equations. We then demonstrate the validity of these equations by comparing predictions with measured data from the study area. Next, we show that the generalized linear relationships are valid for characterizing relationships between nearly all pair combinations of ions. Finally, we explore model sensitivity to assumed upstream end member concentration.

Generalized Linear Relationships Between Ion Concentrations and Salinity

For regions that are dominated by two water sources, we would expect to observe EC values and ion concentrations that are bounded by the respective source values; we would also expect to observe ionic proportions that are characterized by a linear combination (or "mix") of the two sources. One can derive salinity constituent mixing relationships for an estuary with one upstream "fresh" water source and one downstream "saline" water source (Loder and Reichard 1981) for each constituent. Consider the following mixing relationships for ionic constituent i and salinity:

$$C_{i,n} = C_{i,s} * M_n + C_{i,f} * \left(1 - M_n\right) \tag{2}$$

$$S_n = S_s * M_n + S_f * \left(1 - M_n\right) \tag{3}$$

where $C_{i,n}$ represents the concentration of ionic constituent i for a given sample n, $C_{i,s}$ and $C_{i,f}$ are ionic constituent i end member concentrations for seawater and freshwater, respectively, S_n represents the practical salinity value for a given sample n, S_s and S_f are the end member practical salinity values for seawater and freshwater, respectively, and M_n represents the seawater mixing ratio ($0 \le M_n \le 1$) for a given sample n.

Substituting Eq. (3) into Eq. (2), combining terms and solving for $C_{i,n}$ result in the following relationship between ion concentration and practical salinity for a given sample n:

$$C_{i,n} = A_i * S_n + B_i \tag{4}$$

where the slope A_i (a proportionality constant) and intercept B_i are expressed by Eqs. (5) and (6) below:

$$A_i = \frac{\left(C_{i,s} - C_{i,f}\right)}{\left(S_s - S_f\right)} \tag{5}$$

$$B_i = C_{i,f} - \left(A_i * S_f\right) \tag{6}$$

Assuming the sum of major ions for sample n, when measured in units of ppt, is approximately equal to practical salinity yields:

$$\sum_i A_i \approx 1 \tag{7}$$

$$\sum_i B_i \approx 0 \tag{8}$$

We note that the above steady state conservative mixing approach, while presented as functions of practical salinity, can also be applied to represent relationships between various ions (e.g., estimating Br^- concentration as a function of Cl^- concentration). We also note that, although the upstream end member of the San Francisco estuary is not truly a single source water, the assumption of single source is generally sufficient.

Derivation of the PSS-78 Extension

The proposed extension of PSS-78 to estimate the concentrations of ionic constituent i as a function of the conductivity ratio is derived by substituting Eq. (1) into Eq. (4), resulting in:

$$C_i = J_{io} + J_{i1} * R^{0.5} + J_{i2} * R + J_{i3} * R^{1.5} + J_{i4} * R^2 + J_{i5} * R^{2.5} \tag{9}$$

where

$$J_{i0} = A_i * K_0 + B_i \tag{10}$$

$$J_{i1} = A_i * K_1 \tag{11}$$

$$J_{i2} = A_i * K_2 \tag{12}$$

$$J_{i3} = A_i * K_3 \tag{13}$$

$$J_{i4} = A_i * K_4 \tag{14}$$

$$J_{i5} = A_i * K_5 \tag{15}$$

and

$$\sum_{e=0}^{5} J_{ie} = C_{i,s} \forall\ i \tag{16}$$

Application of PSS-78 Extension to Study Area

Results of an application of the PSS-78 extension to the study area are reported below in concentration units of mg/L for the various ions. We assumed equivalence between dimensionless practical salinity units from Eq. (1) and salinity concentration in ppt, acknowledging small differences between the two (Millero et al. 2007). Appropriate density adjustments were made to translate from ppt to mg/L.

End Member Concentrations

Table 2 summarizes end member concentrations proposed for the San Francisco estuary. To improve fidelity of estimated values to the study area's observed data, downstream seawater end member concentrations were determined for each constituent through a sum-of-squares minimization fitting approach to data collected at the three confluence monitoring locations (D10A, D10, and D15) rather than using published values for standard seawater. Specifically, this fitting approach attempted to minimize the difference between predicted and observed ion concentrations. Reported ion and TDS values are within 4% of seawater values reported by Riley and Skirrow (1965). The downstream seawater end member EC value of 52,300 µS/cm was also determined through a sum-of-squares minimization fitting approach (Hutton and Roy in review). Upstream freshwater end member concentrations were generally determined for each constituent through a least-squares regression approach, assuming (i) a quadratic fit applied to samples with EC ranging between 250 and 1000 µS/cm (Hutton et al. 2022b) and (ii) the upstream end member is represented by an EC = 250 µS/cm. This data subset represents 15% of the data measured at D10, D10A, and D15 with EC ≥ 250 µS/cm. Resulting end member concentrations were checked for appropriate charge balance between anions and cations. Table 2 provides end member anion and cation sums in milliequivalents per liter (meq/L).

Average annual inflows to the Delta from the Sacramento and San Joaquin Rivers are approximately 30 and 4 billion cubic meters, respectively (https://data.cnra.ca.gov/dataset/dayflow). Given this stark difference in flows, we would expect the ionic makeup of the confluence region (i.e., upstream end member) to be more reflective of Sacramento River water than San Joaquin River water during periods of minimal salinity intrusion from the Pacific Ocean. And since much of the San Joaquin River inflow does not reach the confluence due to out-of-basin exports and in-Delta agricultural and urban diversions, the relative inflow contribution from the Sacramento River at the confluence is even greater than indicated by the inflow proportion. However, this simplistic observation belies the fact that the ionic makeup of the confluence region (i.e., upstream end member) generally reflects a blend of Sacramento and San Joaquin River water—possibly due to the influence of agricultural drainage in the region.

Table 2 End member baseline and sensitivity values

Salinity constituent	Units	Downstream baseline value (seawater)	Upstream baseline value (freshwater)	High alkalinity upstream value	Low alkalinity upstream value
EC	µS/cm	52,300	250	250	250
TDS	mg/L	36,300	145	145	145
Br^-	mg/L	67	0.09	0.05	0.12
Cl^-	mg/L	19,630	25	16	38
SO_4^{2-}	mg/L	2,660	17	16	19
Alkalinity	mg/L as $CaCO_3$	119	67	80	47
Na^+	mg/L	10,600	22	17	26
Ca^{2+}	mg/L	420	14	16	12
Mg^{2+}	mg/L	1,295	9	8	10
K^+	mg/L	405	2.0	2.0	2.0
Practical salinity	Dimensionless	35	0.122	0.122	0.122
Anion sum	meq/L	612	2.4	2.4	2.4
Cation sum	meq/L	599	2.5	2.3	2.6

Model Constants

The model constants associated with Eq. (9) are summarized in Table 3 for major ions and TDS. The values reported in this table were computed from Eqs. (5), (6), and (10) thru (15) given PSS-78 fitting constants and end member values reported in Table 2. These model constants are valid for samples with EC ≥ 250 µS/cm. Model predictions from Eq. (9) utilizing constants from Table 3 are not valid under low salinity conditions when EC < 250 µS/cm. Under such conditions, waters in the study area overwhelmingly reflect characteristics of upstream freshwater flows and do not reflect seawater mixing. Using a least-squares regression approach, we applied a quadratic adjustment to the model that constrained modified concentration estimates to equal unmodified concentration estimates at EC = 250 µS/cm, resulting in adjusted values for the $J_{i,0}$, $J_{i,2}$, and $J_{i,4}$ constants. These adjusted values are reported in Table S1 of the Electronic Supplemental Material.

Analysis of Model Residuals

Ion and TDS concentration data from confluence monitoring locations (D10A, D10,and D15) were compared with predicted values from Eq. (9) to access goodness of fit. A frequency analysis of model residuals is summarized in Table S2 of the Electronic Supplemental Material, with the top table providing results for samples with EC ≥ 250 µS/cm and the bottom table providing results for samples with EC < 250 µS/cm. Figure 2 presents scatter plots of ion and TDS concentrations as functions of EC. This figure, which is limited to samples with EC ≥ 250 µS/cm, includes TDS, Cl^-, and alkalinity data from miscellaneous Bay locations downstream of the confluence (see Table 1) and overlays observed data and predicted values.

Predictions are generally very good for samples with EC ≥ 250 µS/cm, with over 90% of estimates within ± 15% of observed values for all constituents except Br^- and alkalinity. For these samples, the model's goodness of fit to alkalinity data is distinctively poorer than for the other constituents over the entire range of EC; this observation is discussed in a subsequent section. For samples with EC < 250 µS/cm, the adjusted model goodness of fit is generally poorer, with approximately 90% of estimates within ± 15% of observed values limited to TDS, alkalinity, Na^+, Ca^{2+}, and Mg^{2+}. Absolute values of the adjusted model residuals frequently exceed 25% for K^+, Br^-, and $SO4^{2-}$ with an apparent bias toward overprediction. We recommend setting Br^- estimates at a constant value of 0.03 mg/L at EC values below 170 µS/cm.

As shown in Fig. S1 in the Electronic Supplemental Material, the normality of model residuals associated with the high salinity data set (EC ≥ 250 µS/cm) was tested using Q-Q plots (which compare sample quantiles of model residuals with the same quantiles from standard normal distributions). The Q-Q plots show reasonable matches with normality in the central part of the distributions, although deviations are apparent at the tails given the range of data over multiple orders of magnitude (note the linear scale for the y-axis in Fig. S1 compared to the log scale in Fig. 2). The Q-Q plots provide additional context for the distribution of the residuals; in particular, the plots suggest most are drawn from distributions that are over-dispersed relative to normal distributions. Importantly, however, the residuals are not derived from fitted regression models, but rather from applications of Eq. (9) using literature-derived fitting constants and assumed end member concentrations.

We also observed evidence of seasonal bias in model residuals (EC ≥ 250 µS/cm), with bias being more pronounced at the lower end of the salinity range. SO_4^{2-}, alkalinity, Ca^{2+}, and Mg^{2+} were generally underpredicted by the model in December thru June and overpredicted by the model in July through November (see Fig. 3). The opposite trend was observed for Br^-, Cl^-, and Na^+. No seasonal bias was observed in the K^+ data. We hypothesize that this observed seasonal bias is related to the simplified assumption of fixed upstream end member concentrations. These findings suggest that the upstream end member concentrations are more reflective of high alkalinity freshwater from the Sacramento River in the wetter December through June season and less reflective of this freshwater source in the drier July thru November season.

Table 3 Extended PSS-78 model constants (see Eq. 9) for samples with EC ≥ 250 µS/cm. Concentrations are reported in mg/L

	TDS	Br^-	Cl^-	SO_4^{2-}	Alkalinity	Na^+	Ca^{2+}	Mg^{2+}	K^+
J_0	30.5249	-0.1246	-36.7037	9.0816	66.8347	-11.5083	12.3481	4.7570	0.6791
J_1	-225.3645	-0.4171	-122.2013	-16.4718	-0.3253	-65.9358	-2.5330	-8.0171	-2.5123
J_2	26,256.2028	48.5929	14,237.1225	1,919.0532	37.8988	7,681.8844	295.1074	934.0329	292.6960
J_3	14,275.9155	26.4207	7,740.9502	1,043.4198	20.6062	4,176.7628	160.4546	507.8486	159.1435
J_4	-6,716.1510	-12.4297	-3,641.7552	-490.8802	-9.6942	-1,964.9717	-75.4864	-238.9190	-74.8696
J_5	2,678.8722	4.9578	1,452.5875	195.7975	3.8667	783.7686	30.1093	95.2977	29.8632
$\sum J$	36,300	67	19,630	2,660	119	10,600	420	1,925	405

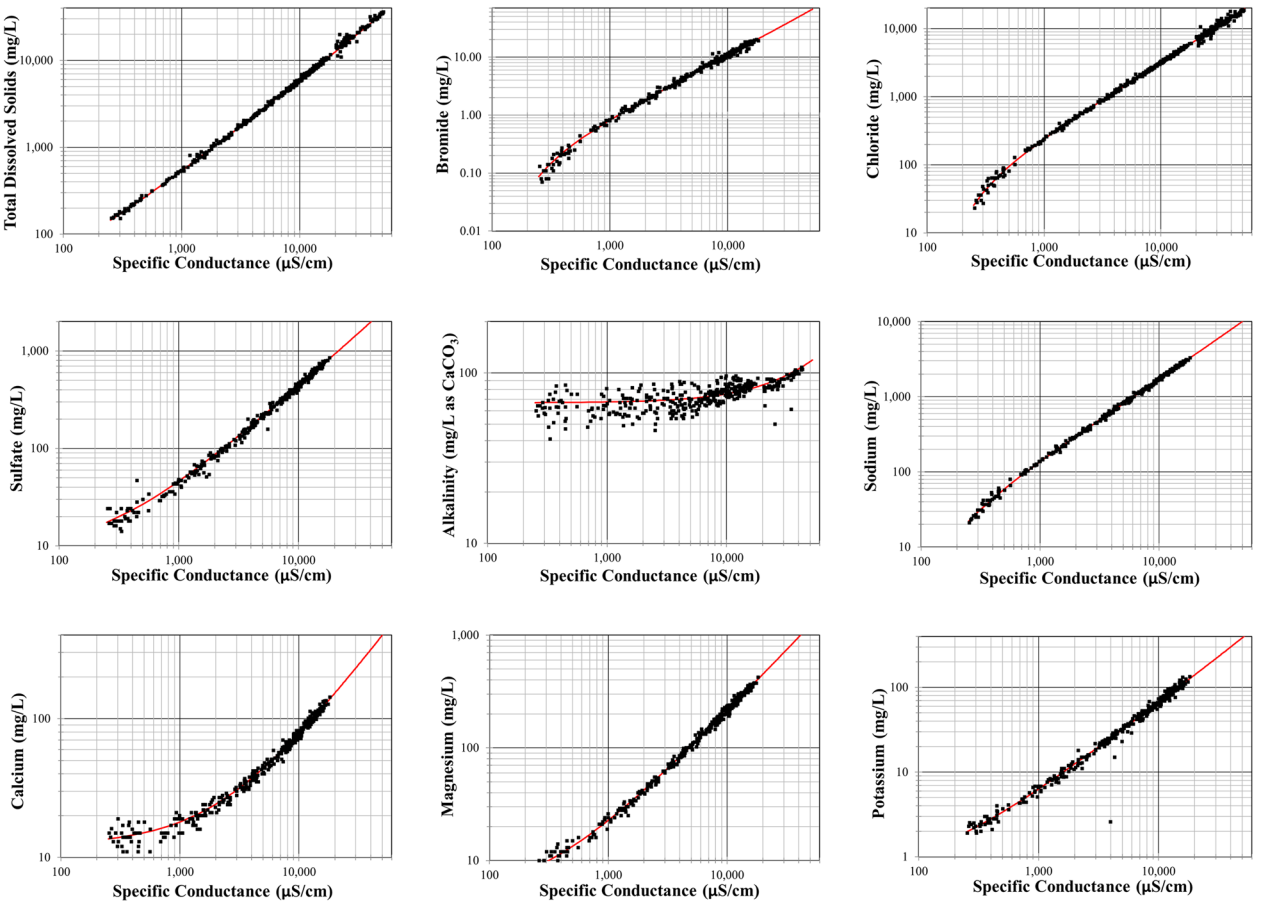

Fig. 2 Predicted and measured ions and TDS as functions of EC

Model Sensitivity to Upstream End Member Concentration

Following our findings of seasonal bias in model residuals, we conducted a sensitivity analysis on assumed upstream end member values reported in Table 2. We evaluated two charge-balanced end members, each with an approximate EC of 250 µS/cm and baseline TDS and K^+ concentrations of 145 and 2 mg/L, respectively. One upstream end member is representative of a higher alkalinity water (generally aligned with the December through June period); a second upstream end member is representative of a lower alkalinity water (generally aligning with the July through November period). The ionic makeup of these two upstream end members are provided in Table 2 alongside the baseline values.

We found model predictions to be locally sensitive to perturbation of the upstream end member concentrations. The perturbed end members generally bounded ion data scatter with EC at levels below 1,000 µS/cm (see Fig. S2 in the Electronic Supplemental Material). However, at higher EC levels, data scatter was generally not well-explained by variation in assumed upstream end member concentration. To illustrate this finding, Fig. S3 in the Electronic Supplemental Material shows model sensitivity results in the higher EC range of 2,000–3,000 µS/cm. Alkalinity posed an exception to these general findings. Alkalinity predictions were found to be extremely sensitive to assumed upstream end member concentration. As shown in Fig. 4, the perturbed end members bounded data scatter with EC over the full range of available alkalinity data. This unique behavior can be attributed to alkalinity's flat concentration gradient relative to the other ions, ranging between 67 mg/L and 119 mg/L for the baseline upstream (freshwater) and downstream (seawater) end members, respectively. To a lesser extent, Ca^{2+} also exhibits a relatively flat concentration gradient, ranging between 14 mg/L and 420 mg/L for the baseline upstream (freshwater) and downstream (seawater) end members, respectively. Due to this flat gradient, Ca^{2+} estimates were found to be more sensitive to assumed upstream end member concentration than the other ions (excluding alkalinity) at higher EC levels (see Fig. S2).

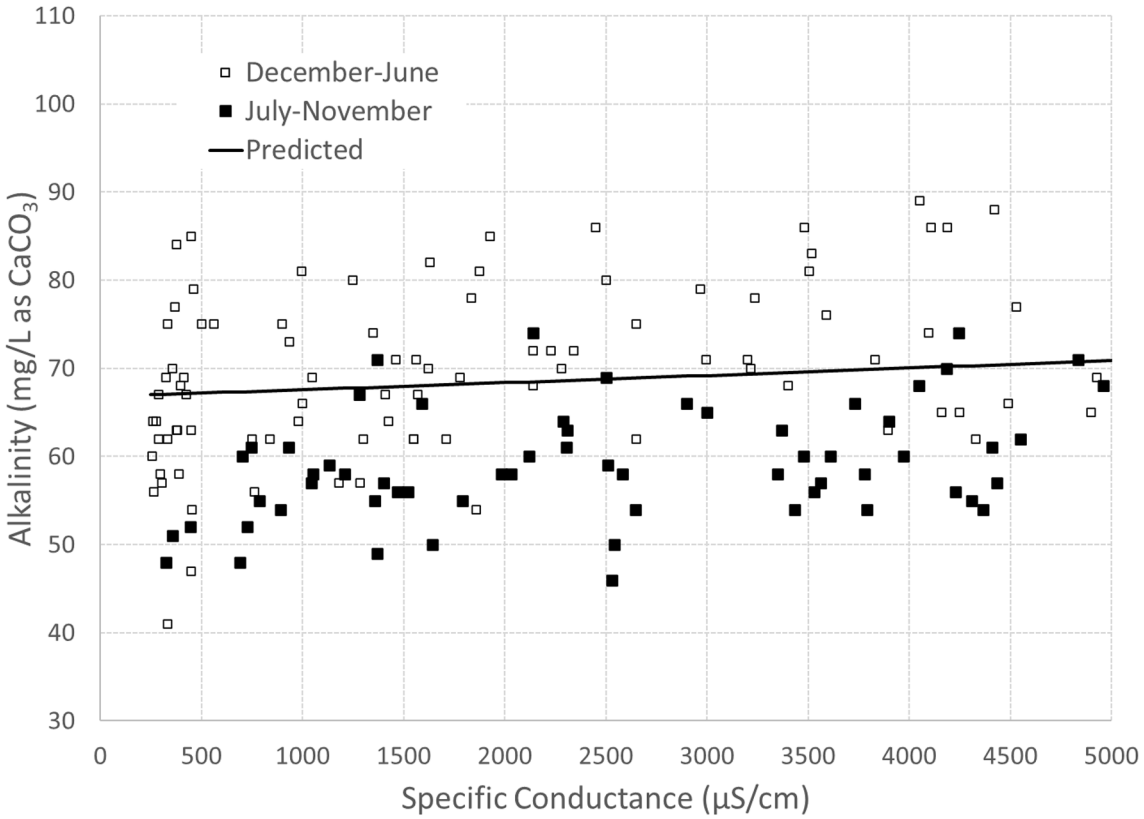

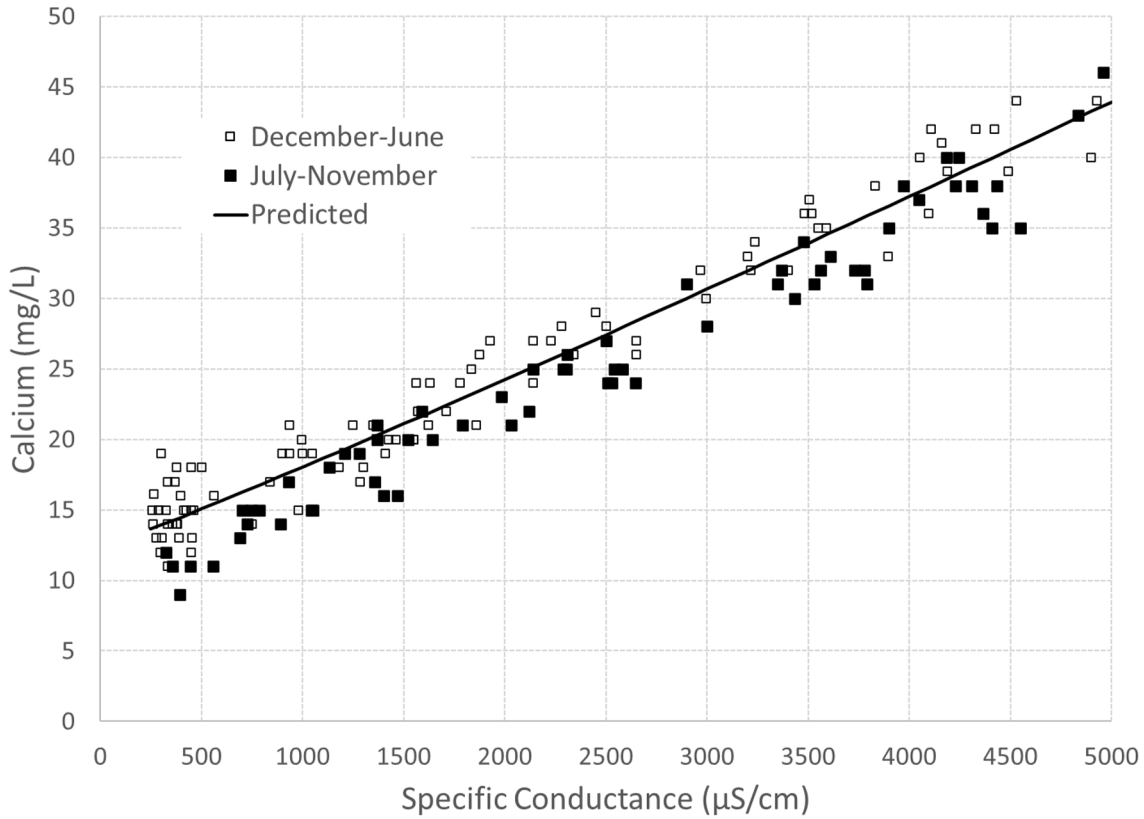

Fig. 3 Seasonal bias in EC scatter plots with alkalinity and calcium

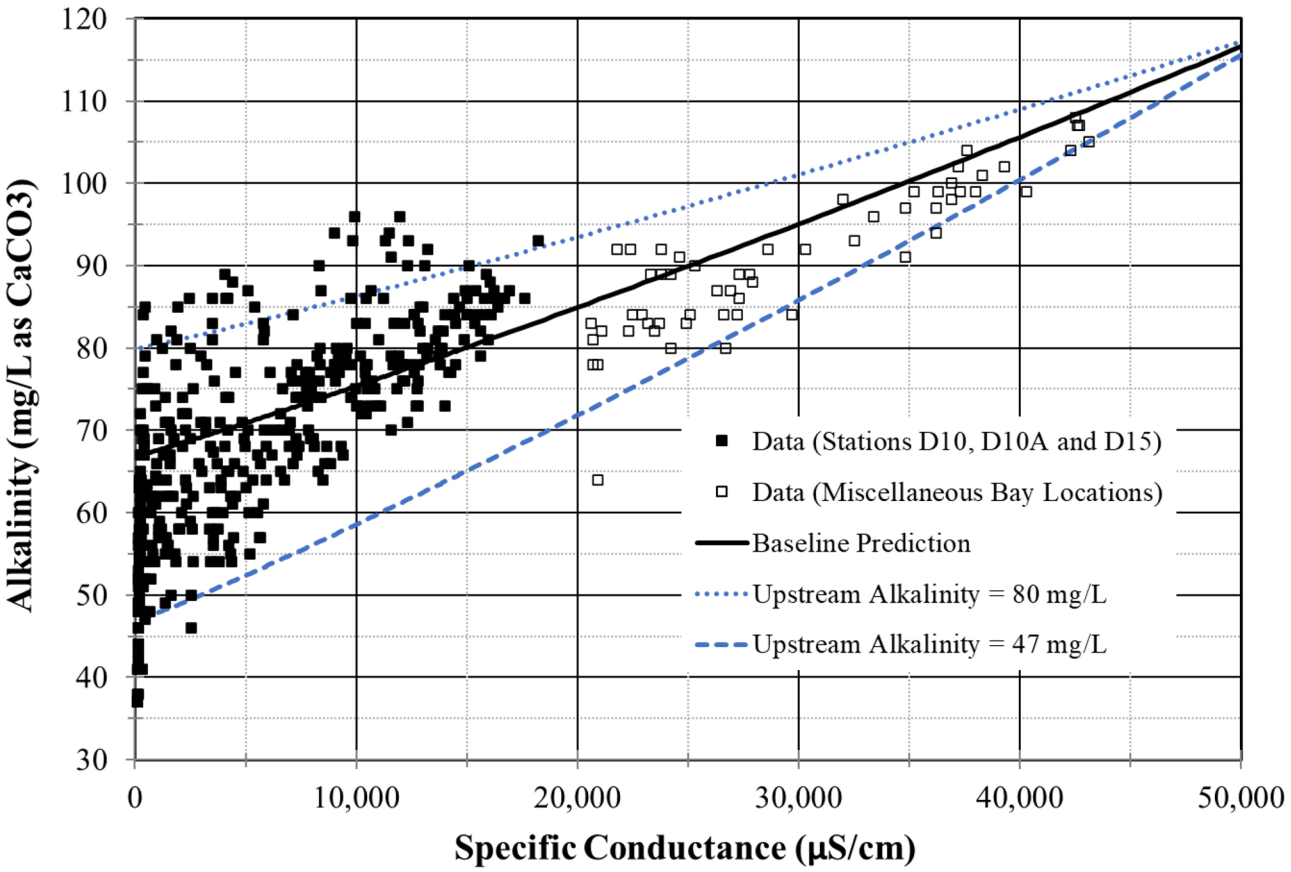

Fig. 4 Sensitivity of alkalinity predictions to assumed upstream end member concentration

Relationships Between Ions

We noted earlier that the steady state conservative mixing approach, while presented as functions of practical salinity, can also be applied to represent relationships between various ions (e.g., predicting Br^- concentration as a function of Cl^- concentration). Model constants and coefficients of variation are summarized in Table S3 of the Electronic Supplemental Material for all pairs of ions as well as TDS for conditions when EC ≥ 250 µS/cm. Model constants were calculated from Eqs. (5) and (6) assuming baseline downstream and upstream end member concentrations. We observe that the slopes computed from Eq. (5) are approximately equal to the ionic ratios associated with seawater due to the downstream end member values being much greater than the upstream end member values. The reported coefficients of variation suggest that TDS, Cl^-, and Na^+ are the most effective independent variables for predicting ion concentrations. Specifically, Cl^- is the most effective independent variable in predicting Br^-, SO_4^{2-}, and Na^+, while Na^+ is the most effective independent variable in predicting TDS, Cl^-, Mg^{2+}, and K^+. TDS, while not the most effective in predicting any one ion, provides good estimates across the suite of ions. Notably, Mg^{2+} is the most effective independent variable in predicting Ca^{2+}. Similar to its relationship with conductivity ratio, we found alkalinity, as a dependent variable, to be weakly correlated with ions and TDS. However, we did not find alkalinity to correlate as an independent variable. Aligned with our finding of seasonal bias in model predictions, we note that correlations between ions could be improved by seasonal binning; however, detailed analysis of such binning was beyond the scope of our work.

Discussion

This work presents a novel approach to estimate major ion concentrations in estuaries from a known specific conductance through an extension of the Practical Salinity Scale 1978 and application of the assumption of steady state two-source conservative mixing. This method, which builds conceptually on the mixing diagram widely used for interpreting the transport of conservative and non-conservative constituents in estuaries (e.g. Maeda 1952; Loder and Riechard 1981; Wong 1979; and other more recent studies), has a similar broad application to other estuaries which

can be approximated by two sources of salinity—one seawater and one freshwater. Using observed ionic constituent and specific conductance data at the two end members, the approach employed here can be directly used to estimate ionic concentrations from specific conductance measurements all along the estuarine salinity gradient. The general methodology, as well as limitations outlined below, although focused on San Francisco estuary, are applicable to other estuarine settings with similar data availability.

Using an extensive salinity data set, we demonstrated the model's validity and limitation for the San Francisco estuary when specific conductance values are ≥ 0.25 mS/cm and developed adjusted model constants to account for ionic composition under less saline conditions. We observed evidence of seasonal bias in model residuals and hypothesize that this bias is related to the simplified assumption of fixed upstream end member concentrations. This finding of seasonal bias suggests that upstream end member concentrations are more reflective of high alkalinity freshwater contributions in the December through June season and less reflective of this freshwater source in the July through November season.

The approach presented here offers advantages over least-squares regression-based approaches for characterizing relationships between ion concentrations and specific conductance in an estuarine environment. One key advantage of this approach is that, since it relies on conservative mixing assumptions rather than regression, it does not have significant data requirements for model calibration at individual locations across the salinity gradient. For our study, this was an important advantage as measured data were sparse at conductance levels greater than 17,000 µS/cm. Another key advantage of this approach is that it provides a quasi-mechanistic framework for interpreting the influence of variations in freshwater inputs on salinity relationships. In our examination of the San Francisco estuary, we found weak correlation between alkalinity and specific conductance. By accounting for seasonal variation in the upstream end member concentration, much of this apparent data scatter could be attributed to freshwater inputs rather than measurement uncertainty.

An important limitation of the approach presented here is that it assumes one significant freshwater inflow to the estuary. The San Francisco estuary receives most of its freshwater inflow from two riverine sources—the Sacramento River and the San Joaquin River. For purposes of this work, we defined the approximate upstream boundary of the study area near the confluence of these two rivers. Thus, we assumed the composite flow from these sources to be a single source. Our approach requires significant adaptation for application to regions of the Sacramento-San Joaquin River Delta significantly upstream of the river confluence. Similarly, for estuaries with two or more freshwater tributaries that are not confluent, significant adaptation of this approach would be required.

Another important limitation of the approach presented here is that it assumes that the upstream end member is adequately characterized by PSS-78. Hutton and Roy (in review) show that freshwater inflows from the Sacramento River are well-characterized by PSS-78; however, waters from the San Joaquin River and agricultural drainage are not. In the confluence region, the Sacramento River is volumetrically dominant and thus dilutes the influence of the other sources. However, in regions of the Delta significantly upstream of the river confluence, this issue limits the applicability of the approach.

In estuarine settings, depending on the prevailing beneficial uses, there may be a need to estimate the concentrations of one or more individual salinity constituents from EC measurements. Although location-specific empirical relationships between ion concentration and EC are one approach that has been used, such an approach offers no straightforward way to represent variability across the salinity gradient caused by variations in the freshwater end-member constituent concentrations. The effect is notable for freshwater inflows that have distinct ionic signatures from ocean water. The two-source mixing approach presented here addresses this source of variation, is simple to adapt to other estuaries, and provides a more general framework to relate ionic concentrations along the salinity gradient to EC measurements. Exploration of this methodology across other estuaries is recommended, especially for estuaries that are dominated by a single freshwater inflow.

Supplementary Information The online version contains supplementary material available at https://doi.org/10.1007/s12237-023-01211-z.

Acknowledgements The authors acknowledge the valuable contributions of John Rath (Q-Q plot analysis) and Arushi Sinha (data assembly and screening).

Funding Funding for this work was provided by the State Water Contractors MWQI Specific Projects Committee.

Data Availability All data used in this analysis are available from the corresponding author.

References

Boyle, E., R. Collier, A.T. Dengler, J.M. Edmond, A.C. Ng, and R.F. Stallard. 1974. On the chemical mass-balance in estuaries. *Geochimica et Cosmochimica Acta* 38: 1719–1728.

California Department of Public Works. 1931. Bulletin 27. Variation and control of salinity in the Sacramento-San Joaquin Delta and Upper San Francisco Bay. https://www.waterboards.ca.gov/waterrights/water_issues/programs/bay_delta/deltaflow/docs/exhibits/ccwd/spprt_docs/ccwd_dpw_1931.pdf.

California Department of Water Resources (CDWR). 2003. Water supply contract between the State of California Department of Water Resources and The Metropolitan Water District of Southern California, October 24. Available at: https://calisphere.org/item/ark:/86086/n22f7mgf/.

Carol, E.S., and E.E. Kruse. 2012. Hydrochemical characterization of the water resources in the coastal environments of the outer Río de la Plata estuary, Argentina. *Journal of South American Earth Sciences* 37: 113–121.

CSWRCB (California State Water Resources Control Board). 1999. Water right decision 1641. http://www.swrcb.ca.gov/waterrights/board_decisions/adopted_orders/decisions/d1600_d1649/wrd1641_1999dec29.pdf.

Cloern, J.E., A.D. Jassby, T.S. Schraga, E. Nejad, and C. Martin. 2017. Ecosystem variability along the estuarine salinity gradient: examples from long-term study of San Francisco Bay. *Limnology and Oceanography* 62. https://doi.org/10.1002/lno.10537

Denton, R.A. 2015. Delta salinity constituent analysis, report prepared for the State Water Contractors Authority, Feb. Available online at: https://rtdf.info/.

Dyer, K.R. 1997. *Estuaries: a physical introduction*, 2nd ed. Chichester: John Wiley and Sons/Wiley & Sons.

Hill, K.D., T.M. Dauphinee, and D.J. Woods. 1986. The extension of the Practical Salinity Scale 1978 to low salinities. *IEEE Journal of Oceanic Engineering* OE-11(1).

Howland, R.J.M., A.D. Tappin, R.J. Uncles, D.H. Plummer, and N.J. Bloomer. 2000. Distributions and seasonal variability of pH and alkalinity in the Tweed Estuary, UK. *Science of the Total Environment* 251: 125–138.

Hutton, P.H., and F.I. Chung. 1992. Simulating THM formation potential in Sacramento Delta: part I. *Journal Water Resources Planning & Management, ASCE* 118 (5).

Hutton, P.H., J. Rath, L. Chen, M.L. Ungs, and S.B. Roy. 2015. Nine decades of salinity observations in the San Francisco Bay and Delta: Modeling and trend evaluation. *Journal of Water Resources Planning and Management*. https://doi.org/10.1061/(ASCE)WR.1943-5452.0000617.

Hutton, P.H., and S.B. Roy. in review. Application of the practical salinity scale to the waters of San Francisco estuary.

Hutton, P.H., S.B. Roy, S.W. Krasner, and L. Palencia. 2022a. The municipal water quality investigations program: a retrospective overview of the program's first three decades. *Water* 14: 3426. https://doi.org/10.3390/w14213426.

Hutton, P.H., A. Sinha, and S.B. Roy. 2022b. Simplified approach for estimating salinity constituent concentrations in the San Francisco estuary & Sacramento-San Joaquin River Delta: a user guide, report prepared for the State Water Contractors, July. Available online at: https://rtdf.info/.

Kennish, M.J. 2021. Drivers of change in estuarine and coastal marine environments: an overview. *Open Journal of Ecology* 11 (3): 224–239.

Kimmerer, W. 2005. Long-term changes in apparent uptake of silica in the San Francisco estuary. *Limnology and Oceanography* 50 (3). http://www.jstor.org/stable/3597580.

Krasner, S.W., and G.L. Amy. 1995. Jar-test evaluations of enhanced coagulation. *Journal-American Water Works Association* 87 (10): 93.

Lewis, E.L. 1980. The Practical Salinity Scale 1978 and its antecedents. *IEEE Journal of Oceanic Engineering* OE-5 (1).

Loder, T.C., and R.P. Reichard. 1981. The dynamics of conservative mixing in estuaries. *Estuaries* 4 (1): 64–69.

Maeda, H. 1952. The relation between chlorinity and silicate concentration of water observed in some estuaries. *Publications of the Seto Marine Biological Laboratory* 2 (2): 249–255.

Merrifield, M.S., E. Hines, X. Liu, and M.W. Beck. 2011. Building regional threat-based networks for estuaries in the Western United States. *PLoS ONE* 6 (2): e17407.

Millero, F.J., R. Feistel, D.G. Wright, and T.J. McDougall. 2007. The composition of standard seawater and the definition of the reference-composition salinity scale. *Deep-Sea Research I* 55: 50–72.

Najjar, R. G., M. Herrmann, S.M. Cintrón Del Valle, J.R. Friedman, M.A.M. Friedrichs, L.A. Harris, E.H. Shadwick, E.G. Stets, and R.J. Woodland. 2019. Alkalinity in tidal tributaries of the Chesapeake Bay. *Journal of Geophysical Research: Oceans* 125: e2019JC015597. https://doi.org/10.1029/2019JC015597.

Najm, I.N., and S.W. Krasner. 1995. Effects of bromide and NOM on by-product formation. *Journal-American Water Works Association* 87 (1): 106.

Patra, S., C.Q. Liu, F.S Wang, S. Li, and B.L. Wang. 2012. Behavior of major and minor elements in a temperate river estuary to the coastal sea. *International Journal of Environmental Science and Technology, October*. https://doi.org/10.1007/s13762-012-0097-8.

Reid, G.K., and R.D. Wood. 1976. *Ecology of inland waters and estuaries*, 2nd ed. New York: D. Van Nostrand.

Riley, J.P., and G. Skirrow. 1965. *Chemical oceanography*, vol. 1. London and New York: Academic Press.

Schemel, L. 2001. Simplified conversions between specific conductance and salinity units for use with data from monitoring stations. *Interagency Ecological Program Newsletter* 14 (1).

Sundaray, S.K., B.B. Nayak, and D. Bhatta. 2009. Environmental studies on river water quality with reference to suitability for agricultural purposes: Mahanadi River estuarine system, India–a case study. *Environmental Monitoring and Assessment* 155 (1): 227–243.

Telesh, I.V., and V.V. Khlebovich. 2010. Principal processes within the estuarine salinity gradient: a review. *Marine Pollution Bulletin* 61 (4–6): 149–155.

Wagner, E.D., and M.J. Plewa. 2017. CHO cell cytotoxicity and genotoxicity analyses of disinfection by-products: an updated review. *Journal of Environmental Sciences* 58: 64–76.

Warner, T.B. 1972. Mixing model prediction of fluoride distribution in Chesapeake Bay. *Journal of Geophysical Research* 77 (15).

Wong, G.T.F. 1979. Alkalinity and pH in the Southern Chesapeake Bay and the James River Estuary. *Limnology and Oceanography* 24 (5): 970–977. https://doi.org/10.4319/lo.1979.24.5.0970.

Yarish, C., P. Edwards, and S. Casey. 1980. The effects of salinity, and calcium and potassium variations on the growth of two estuarine red algae. *Journal of Experimental Marine Biology and Ecology* 47 (3): 235–249.

Zhang, Z., Z. Cao, P. Grasse, M. Dai, L. Gao, H. Kuhnert, M. Gledhill, C.M. Chiessi, K. Doering, and M. Frank. 2020. Dissolved silicon isotope dynamics in large river estuaries. *Geochimica et Cosmochimica Acta* 273: 367–382. https://doi.org/10.1016/j.gca.2020.01.028.